Catalytic Nonoxidation Dehydrogenation of Ethane Over Fe-Ni Catalysts Supported on Mg(Al)O to Produce Hydrogen and Easily Purified Carbon Nanotubes

ARTICLE *in* ENERGY & FUELS · NOVEMBER 2007

Impact Factor: 2.79 · DOI: 10.1021/ef7004018

8 AUTHORS, INCLUDING:

Naresh Shah
University of Kentucky
135 PUBLICATIONS **2,777** CITATIONS
SEE PROFILE

Frank Huggins
University of Kentucky
271 PUBLICATIONS **5,272** CITATIONS
SEE PROFILE

Mohindar Seehra
West Virginia University
313 PUBLICATIONS **5,011** CITATIONS
SEE PROFILE

Gerald P Huffman
University of Kentucky
233 PUBLICATIONS **4,842** CITATIONS
SEE PROFILE

Catalytic Nonoxidative Dehydrogenation of Ethane over Fe–Ni and Ni Catalysts Supported on Mg(Al)O to Produce Hydrogen and Easily Purified Carbon Nanotubes

Wenqin Shen,*,† Yuguo Wang,†,‡ Xuebei Shi,† Naresh Shah,† Frank Huggins,† Shilpa Bollineni,§ Mohindar Seehra,§ and Gerald Huffman†

Consortium for Fossil Fuel Science, University of Kentucky, Lexington, Kentucky 40506-0043; Research & Development Center, Saudi Aramco, Dhahran 31311, Saudi Arabia; and Physics Department, West Virginia University, Morgantown, West Virginia 26506

Received July 12, 2007. Revised Manuscript Received September 12, 2007

Nonoxidative decomposition of ethane was conducted over monometallic Ni and bimetallic Fe–Ni catalysts on basic Mg(Al)O support to produce H_2 free of CO and CO_2 and easily purified carbon nanotubes, a potentially valuable byproduct. The Mg(Al)O support was prepared by calcination of synthetic MgAl–hydrotalcite with a Mg to Al ratio of 5. The catalysts were prepared by incipient wetness with total metal loadings of 5 wt %. The dehydrogenation of undiluted ethane was conducted at temperatures of 500, 650, and 700 °C. At 500 °C, the Ni/Mg(Al)O catalyst was highly active and very stable with 100% conversion of ethane to 20 vol % H_2 and 80 vol % CH_4. However, the bimetallic Fe–Ni/Mg(Al)O exhibited its best performance at 650 °C, yielding 65 vol % H_2, 10 vol % CH_4, and 25 vol % unreacted ethane. The product carbon was in the form of carbon nanotubes (CNT) at all three reaction temperatures, but the morphology of the CNT depended on both the catalyst composition and reaction temperature. The CNTs were formed by a tip-growth mechanism over the Mg(Al)O supported catalysts and were easily purified by a one-step dilute nitric acid treatment. Mössbauer spectroscopy, X-ray absorption fine structure spectroscopy, N_2 adsorption–desorption isotherms, TEM, STEM, TGA, and XRD were used to characterize the catalysts and the CNT, revealing the catalytic mechanisms.

1. Introduction

An energy economy based on hydrogen could alleviate growing concerns about energy supply, air pollution, and greenhouse gas emissions. Currently, the most widely used method of hydrogen production is steam reforming or partial oxidation of fossil fuels, particularly natural gas, followed by the water gas shift reaction (WGS) and separation and purification steps. However, the hydrogen purity requirement for use in polymer electrolyte membrane (PEM) fuel cells is demanding (<10 ppm CO), since CO is a poison for the catalysts used in PEM fuel cells. Additionally, the steam reforming-WGS process produces significant amounts of CO_2, a gas believed to contribute to global warming. Therefore, direct, nonoxidative decomposition of hydrocarbons into hydrogen and carbon is an attractive alternative method of producing hydrogen that is free of CO and CO_2. Moreover, the process is a simple one-step reaction:

$$C_xH_y \rightarrow xC + (y/2)H_2 \quad (1)$$

Previous work by our research group has shown that binary Fe–M (M = Ni, Mo, or Pd) catalysts prepared by incipient wetness or coprecipitation on γ-alumina supports have excellent activity for dehydrogenation of methane, ethane, propane, and cyclohexane.[1–3] Results from Mössbauer and XAFS spectroscopies suggest that the active phase is an austenic Fe–M–C alloy that is bound to the alumina support by hercynite ($FeAl_2O_4$).[4,5] The carbon produced by the reaction was present as potentially valuable carbon nanotubes (CNT), which were in the form of multiwalled nanotubes (MWNT) in the most active temperature range. However, the CNT were very difficult to clean because of the limited solubility of alumina and the strong binding of the nanotubes to the support caused by the formation of $FeAl_2O_4$ during the reaction.

To obtain high-quality CNT by the catalytic chemical vapor deposition (CCVD) method requires almost complete removal of the catalyst particles and support. A number of different approaches and purification methods have been developed.[6–11]

* Corresponding author: Tel 1-859-257-6087; Fax 1-859-257-7215; e-mail wshen1@engr.uky.edu.
† University of Kentucky.
‡ Saudi Aramco.
§ West Virginia University.

(1) Shah, N.; Panjala, D.; Huffman, G. P. *Energy Fuels* **2001**, *15*, 1528–1534.
(2) Shah, N.; Wang, Y.; Panjala, D.; Huffman, G. P. *Energy Fuels* **2004**, *18*, 727–735.
(3) Wang, Y.; Shah, N.; Huffman, G. P. *Catal. Today* **2005**, *99*, 359–364.
(4) Shah, N.; Pattanaik, S.; Huggins, F. E.; Panjala, D.; Huffman, G. P. *Fuel Process. Technol.* **2003**, *83*, 163–173.
(5) Punnoose, A.; Shah, N.; Huffman, G. P.; Seehra, M. S. *Fuel Process. Technol.* **2003**, *83*, 263–273.
(6) Fan, Y.-Y.; Kaufmann, A.; Mukasyan, A.; Varma, A. *Carbon* **2006**, *44*, 2160–2170.
(7) Dillon, A. C.; Gennett, T. K.; Jones, M.; Alleman, J. L.; Parilla, P. A.; Heben, M. J. *Adv. Mater.* **1999**, *11*, 1354–1358.
(8) Tohji, K.; Takahashi, H.; Shinoda, Y.; Shimizu, N.; Jeyadevan, B.; Matsuoka, I. *J. Phys. Chem. B* **1997**, *101*, 1974–1978.
(9) Hou, P. H.; Bai, S.; Yang, Q. H.; Liu, C.; Cheng, H. M. *Carbon* **2002**, *40*, 81–85.
(10) Kernadi, K.; Fonseca, A.; Nagy, J. B.; Bernaerts, D.; Riga, J.; Lucas, A. *Synth. Met.* **1996**, *77*, 31–34.

10.1021/ef7004018 CCC: $37.00
Published on Web 11/03/2007

The conventional catalyst supports, such as alumina, silica, and zeolite, are excellent supports for CNT production by CCVD. However, a multistep purification process is required, which leads to a low CNT yield and may even damage the structure of the CNT. Recently, several investigations have used basic catalyst supports to produce CNT by CCVD because of the facile dissolution of the support in dilute acid. Flahaut et al.[12] used a $Mg_{0.9}Co_{0.1}O$ solid solution prepared by combustion synthesis to crack methane in a hydrogen–methane mixture (18 vol % methane) at a temperature of 1000 °C. The solid product was treated with an HCl solution, and the MgO was completely dissolved. There was still some Co left as Co particles embedded within the CNT. Couteau et al.[13] used $CaCO_3$ as catalyst support for Fe and Co monometallic and bimetallic catalysts for acetylene decomposition at 720 °C. The metallic particles and support could be dissolved by dilute acid (30% HNO_3 or HCl) in one step. The purified MWNT were found to be an excellent catalyst support for Fischer–Tropsch (FT) synthesis.[14]

Here, a basic catalyst support, Mg(Al)O, was prepared by calcination of a synthetic hydrotalcite (HTL) precursor. The product of the calcination has pronounced basic character, high surface area, and good stability toward heat and steam and was easily dissolved in dilute nitric acid. Monometallic Ni and bimetallic Fe–Ni (molar ratio of Fe/Ni = 65/35) nanoscale catalysts were deposited on this support using the incipient wetness method and used for decomposition of undiluted ethane, providing both a high hydrogen yield and an easily purified CNT byproduct.

2. Experimental Section

Catalyst Preparation. Mg_{1-x}–Al_x HTL with a Mg/Al molar ratio of 5 was prepared by coprecipitation at constant pH and temperature.[15] A flow of magnesium nitrate and aluminum nitrate solution with a total cation concentration of 1 M and a flow of solution with 10 mol % excess of KOH and K_2CO_3 (molar ratio of CO_3^{2-} to Al^{3+} equal to 0.5) were pumped into a matrix solution using syringe pumps. The pH value of the matrix solution was controlled to between 8.5 and 9.5 by tuning the syringe pump flow rates. The reaction temperature was controlled at 70 °C. The end point pH was adjusted to 9.5 by adding excess KOH. After reaction, the precipitate was aged overnight at room temperature, then filtered and redispersed in hot deionized water for several cycles to completely wash off any adsorbed K^+ (pH = 7), and finally dried at 100 °C for 24 h. The dried precipitate was then calcined in air at 550 °C for 5 h, cooled to room temperature, and ground into a fine powder (<100 mesh), which was labeled as Mg(Al)O catalyst support.

The catalysts were prepared by incipient wetness method. The catalyst precursors, $Fe(NO_3)_3{\bullet}9H_2O$ and $Ni(NO_3)_2{\bullet}6H_2O$, based on the desired Fe/Ni ratio (65/35) and total metal loading of 5 wt %, were dissolved in deionized water, then mixed with the dry Mg(Al)O powder, and dried in an oven at 80 °C. This was repeated three or four times with a volume of the added solution close to the total pore volume of the support powder each time until the catalyst precursor solution was totally absorbed. The resulting material was then dried in an oven overnight at 80 °C, calcined in air at 550 °C for 5 h, cooled to room temperature, and stored in a dry place.

Ethane Dehydrogenation Reaction. The dehydrogenation reaction was performed in a fixed-bed plug-flow reactor described in detail with a schematic diagram elsewhere.[1] Briefly, the reaction chamber was a quartz tube with an inner diameter of 22.5 mm. One gram of catalyst powder was loaded at the center of the reactor and activated by reduction in hydrogen. The reduction was conducted by heating the furnace slowly at 2 °C/min up to 700 °C and maintaining this temperature under a hydrogen flow rate of 50 mL/min for 2 h. The decomposition reaction was conducted at 500, 650, and 700 °C, with an ethane flow rate of 10 mL/min. The inlet gas flow was controlled by a mass flow controller, and the effluent was monitored by a bubble flow meter and analyzed by online gas chromatography (GC) with a thermal conductivity detector (TCD). The solid product was collected after reaction. The gaseous products were quantified as volume percentages of the total gaseous effluent.

CNT Purification. Nitric acid was used to remove the catalyst from the produced CNT. The collected CNT were purified at room temperature or under reflux in 6 M HNO_3 solution for 2 h. The material was filtered and then thoroughly washed using deionized water to remove the adsorbed HNO_3. The purified CNT were then dried in an oven at 80 °C overnight.

Catalyst Characterization. The N_2 adsorption–desorption isotherms were measured for the Mg(Al)O support, and the catalysts in their as-prepared and reduced conditions at liquid nitrogen temperature on a Micromeretics TRISTAR 3000 instrument. Prior to the adsorption and desorption measurement, the samples were degassed overnight at 150 °C with a N_2 purge. Powder X-ray diffraction was conducted on a Siemens 5000 diffractometer using Ni-filtered Cu Kα radiation and a scanning rate of 0.5° 2θ min^{-1}. The Mg(Al)O support grain size was calculated from the full width at half-maximum (fwhm) of the principal peaks, using the Debye–Scherrer equation. The morphologies of the catalysts and the produced CNT were characterized by transmission electron microscopy (TEM) using a JEOL 2010F instrument at a voltage of 200 kV. TEM samples were prepared by crushing the samples, dispersing them in acetone by ultrasonication for 15 min, loading a single drop of the suspension onto lacey carbon TEM grids, and drying the grids at room temperature for 10 min. ^{57}Fe Mössbauer spectroscopy was used to characterize the atomic structure of the Fe–Ni catalyst on the Mg(Al)O support, while X-ray absorption spectroscopy was used to characterize the Ni/Mg(Al)O catalyst. Thermal gravimetric analysis was carried out in a 100 mL/min flow rate of air to measure the purity of the produced and purified CNT. The heating rate was 10 °C/min from room temperature to 950 °C.

3. Results and Discussion

Properties of Mg(Al)O Support and Catalysts. Hydrotalcite (HTL) compounds, also known as layered double hydroxides (LDH), are natural or synthetic materials with the general formula of $[M^{2+}_{1-x}M^{3+}_x(OH)]A^{n-}_{x/n}{\bullet}mH_2O$, where M^{2+} and M^{3+} represent divalent and trivalent cations in the octahedral sites within the hydroxyl layers, x is equal to the ratio of $M^{3+}/(M^{2+} + M^{3+})$, typically in the range 0.17–0.33, and A^{n-} is the exchangeable interlayer anion, balancing the positive charge on the layers. The $M^{2+}/M^{3+}(OH)_6$ octahedra form two-dimensional sheets that stack together by hydrogen bonding between the hydroxyl groups of adjacent sheets. Usually, synthetic hydrotalcites are reported to have hexagonal structure.[16] In this study, M^{2+} and M^{3+} represent Mg^{2+} and Al^{3+} cations, respectively, and $x = 0.167$.

Figure 1 shows the X-ray powder diffraction patterns of MgAl–HTL as-prepared, the Mg(Al)O catalyst–support prepared by calcination of MgAl–HTL at 550 °C for 5 h, and the as-prepared Fe–Ni/Mg(Al)O catalyst. The XRD pattern of MgAl–HTL exhibits a typical crystalline layered double hy-

(11) Chen, P.; Zhang, H. B.; Lin, G. D.; Hong, Q.; Tsai, K. R. *Carbon* **1997**, *35*, 1495–1501.
(12) Flahaut, E.; Peiney, A.; Laurent, Ch.; Rousset, A. *J. Mater. Chem.* **2000**, *10*, 249–252.
(13) Couteau, E.; Hernadi, K.; Seo, J. W.; Thiên-Nga, L.; Mikó, Cs.; Gaál, R.; Forró, L. *Chem. Phys. Lett.* **2003**, *378*, 9–17.
(14) Bahome, M. C.; Jewell, L. L.; Hildebrandt, D.; Glasser, D.; Coville, N. J. *Appl. Catal., A* **2005**, *287*, 60–67.
(15) Schaper, H.; Berg-Slot, J. J.; Strork, W. H. J. *Appl. Catal.* **1989**, *54*, 79–90.
(16) Bellotto, M.; Rebours, B.; Clause, O.; Lynch, J.; Bazin, D.; Elkaïm, E. *J. Phys. Chem.* **1996**, *100*, 8527–8534.

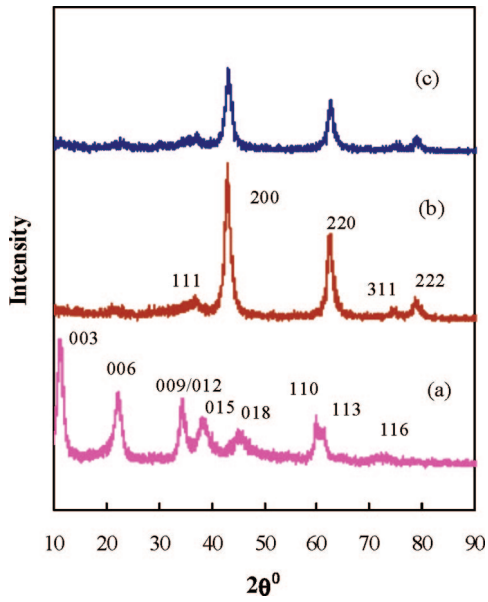

Figure 1. X-ray diffraction patterns of (a) HTL as-prepared, indexed according to JCPDS Card No. 22-700; (b) Mg(Al)O support after calcination of HTL at 550 °C for 5 h, indexed according to JCPDS Card No. 45-0946; and (c) Fe-Ni/Mg(Al)O catalyst as-prepared.

droxide structure with a hexagonal stacking. Kuśtrowski et al.[17] found that the crystallinity of HTL decreased with increasing molar ratio of Mg to Al. In our experiments, we used a Mg to Al molar ratio of 5, which is on the borderline of effective formation of HTL. The crystallite size of the as-prepared MgAl–HTL was calculated from the fwhm of the (018) and (006) reflections using the Debye–Scherrer formula and found to be around 6 nm. Thermal decomposition of HTL leads to a solid solution, which is characterized by a high surface area and homogeneous dispersion of the metal oxides. The XRD pattern of Mg(Al)O after calcination at 550 °C for 5 h shows only the pattern of cubic MgO with high crystallinity due to the fact that aluminum ions also occupy the octahedral sites in the MgO lattice. This special structure has been verified by ^{27}Al solid-state NMR by Schapter et al.[15] The thermal decomposition behavior of MgAl–HTL was studied by Rao et al.[18] using a TG-DTA thermogram. They observed three main stages: (1) the loss of physisorbed and interlayer water below 260 °C, (2) dehydroxylation and removal of carbonate ions between 260 and 500 °C, and (3) the decomposition of $MgCO_3$ above 500 °C. In our experiment, calcination at 550 °C is sufficient for dehydroxylation to form Mg(Al)O oxide with a high surface area. The XRD pattern of the as-prepared Fe–Ni/Mg(Al)O catalyst exhibits no obvious difference from that of the pure Mg(Al)O support, indicating that Fe^{3+} trivalent ions and Ni^{2+} divalent ions are either dispersed in the support or present in oxide particles too small in size and amount to yield a significant diffraction pattern.

The surface areas of the Mg(Al)O support, the Ni/Mg(Al)O catalyst, and the FeNi/Mg(Al)O catalyst, both as-prepared and reduced in hydrogen, are listed in Table 1. It is seen that the surface areas decrease slightly on adding the catalyst precursors, possibly due to interaction between the precursor and the support, and undergo a more significant decrease after reduction

(17) Kuśtrowski, P.; Sułkowska, D.; Chmielarz, L.; łasocha, A. R.; Dudek, B.; Dziembaj, R. *Microporous Mesoporous Mater.* **2005**, *78*, 11–22.

(18) Rao, M. M.; Reddy, B. R.; Jayalakshmi, M.; Jaya, V. S.; Sridhar, B. *Mater. Res. Bull.* **2005**, *40*, 347–359.

Table 1. Surface Areas of the Mg(Al)O Support and the Ni/Mg(Al)O and Fe–Ni/Mg(Al)O Catalysts in As-Prepared and Reduced (under 50 mL/min H_2 at 700 °C for 2 h) States

sample	BET area[a] (m^2/g)	external surface area[a] (m^2/g)
Mg(Al)O support	154	167
Ni/Mg(Al)O as-prepared	114	130
Ni/Mg(Al)O reduced	101	114
FeNi/Mg(Al)O as-prepared	122	137
FeNi/Mg(Al)O reduced	84	94

[a] Note: the error is within 1%.

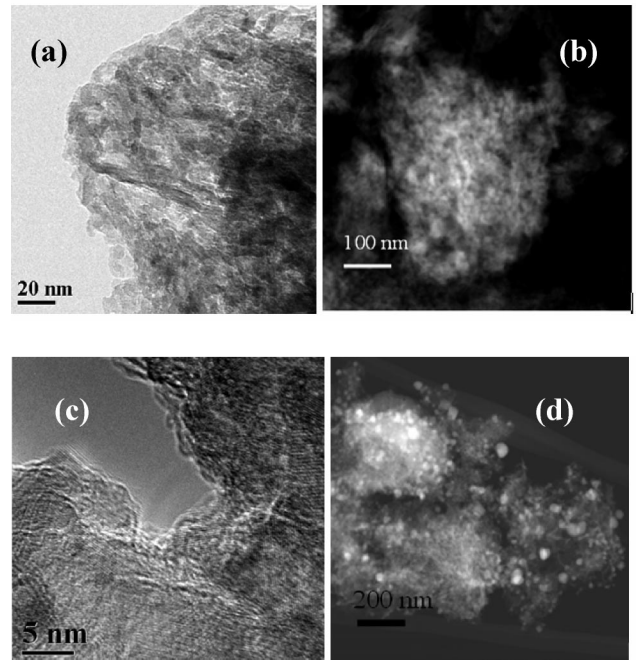

Figure 2. Micrographs of FeNi/Mg(Al)O catalyst: (a) TEM image of the as-prepared catalyst; (b) STEM image of as-prepared catalyst; (c) TEM image of catalyst reduced at 700 °C for 2 h; (d) STEM image of reduced catalyst.

at 700 °C due to sintering of both the support and the catalyst particles. The decrease in surface area during reduction for the Fe–Ni/Mg(Al)O catalyst was ~30%. Schaper et al.[15] investigated the effect of the calcination temperature on the surface area of similar Mg(Al)O compounds and found that increasing temperature from 500 to 700 °C decreased the surface area 20%.

The morphology of the as-prepared and the reduced Fe–Ni/Mg(Al)O catalyst is shown in Figure 2. In the TEM mode (Figure 2a,c), the contrast between catalyst particles and the Mg(Al)O support is relatively weak. However, it clearly shows that the Mg(Al)O support is made up of loosely sintered nanocrystals with particle sizes of the order of 10–20 nm, in rough agreement with the value estimated from the XRD line broadening using the Debye–Scherrer equation. After the catalyst was reduced at 700 °C for 2 h in H_2, some sintering of the support can be seen (Figure 2c). In the STEM mode, (Figure 3d), metallic Fe–Ni catalyst particles having a broad size distribution ranging from small nanoparticles (~10 nm) to relatively large particles (20–40 nm) are clearly observed. No distinct Fe or Ni oxide particles are observed on the as-prepared catalyst (Figure 2b), which indicates that Fe and Ni are well and evenly dispersed prior to reduction. The Ni/Mg(Al)O catalyst shows similar results.

Figure 3 shows the Ni K-edge X-ray absorption near-edge structure (XANES) spectrum and the Fourier transform (FT) of the k^3-weighted extended X-ray absorption fine structure

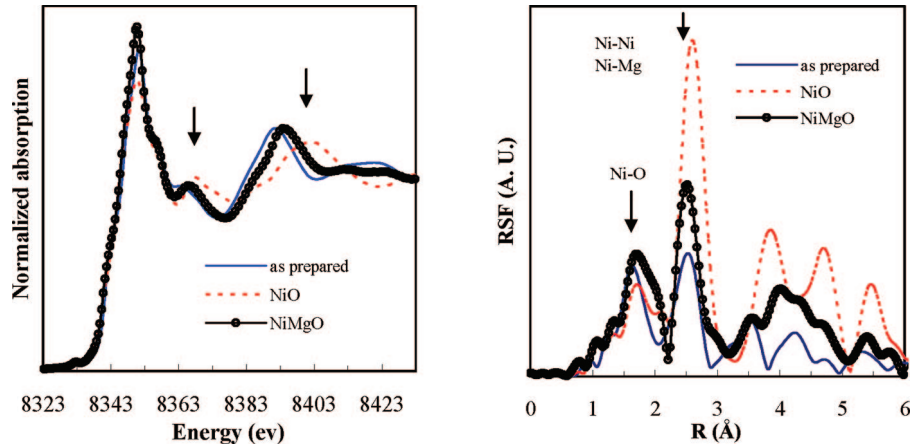

Figure 3. Ni K-edge XANES spectra (left) and Fourier transforms of k^3-weighted Ni K-edge EXAFS (right) of the as-prepared Ni/Mg(Al)O catalyst, NiO, and NiMgO solid solution.

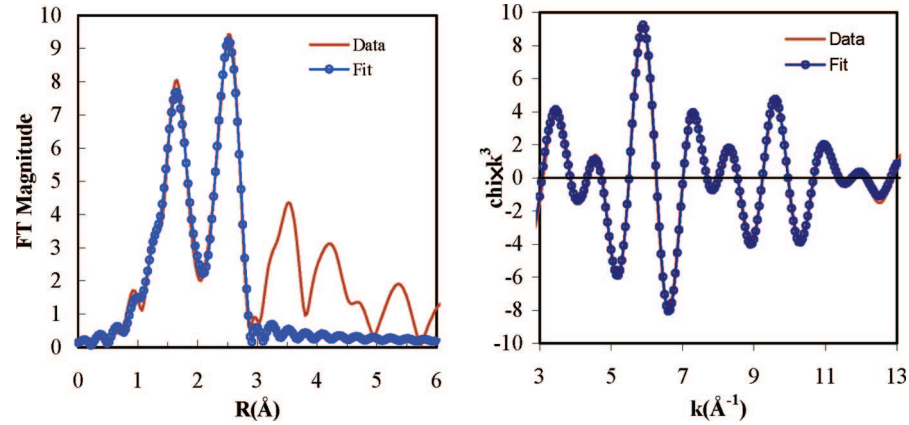

Figure 4. EXAFS spectrum for as-prepared Ni/MgAl(O): radial structure function (left) and the back FT (q) spectrum for the first two shells (right), using the FEFF least-squares analysis.

(EXAFS) of the as-prepared Ni/Mg(Al)O catalyst. The spectra of NiO and NiMgO (Ni:Mg = 1:1, atomic ratio) solid solution are also shown for reference. The XANES spectrum of the as-prepared Ni/Mg(Al)O resembles that of NiMgO in the white-line region. Both the spectra of the as-prepared Ni/Mg(Al)O and NiMgO solid solution have more intense white lines than that of NiO. The peaks at around 8360 and 8400 eV, marked by arrows in Figure 3, shift to lower energy with reduced Ni content and become narrower compared to those of pure NiO.

The radial structure function (RSF) resulting from Fourier transformation of the k^3-weighted EXAFS in the range of 3–13 Å^{-1} of the as-prepared Ni/Mg(Al)O catalyst is also shown in Figure 3 (right). The first peak at ~1.5 Å is due to the backscattering by the nearest oxygen shell, and the second peak is due to backscattering by Ni next-nearest neighbors in the second coordinate shell in pure NiO or by (Mg, Ni) neighbors in Ni/Mg(Al)O catalyst and the NiMgO solid solution. The intensity of the second peak of as-prepared Ni/Mg(Al)O catalyst is much lower than that of NiMgO solid solution, which is likely due to the dilution of Ni in the Mg(Al)O support. Yoshida et al.[19] conducted an in-depth study of the NiO–MgO system by XAFS. It was concluded that a solid solution was formed by impregnation of MgO powder with an aqueous solution of $Ni(NO_3)_2$ followed by calcination at 500 °C over the entire range of Ni concentration. Here, the RSF spectra of the as-prepared Ni/Mg(Al)O catalyst and NiMgO solid solution closely match those of $Ni_xMg_{1-x}O$ compounds with x equal to 0.02 and 0.48, respectively, as observed by Yoshida et al.[19] This similarity indicates that all the Ni in the as-prepared Ni/Mg(Al)O catalyst is incorporated into octahedral sites in the Mg(Al)O lattice. To confirm this conclusion, FEFF EXAFS analysis was performed in R-space over the range 1–3 Å, which includes only the first two coordination shells. The combined coordination number for the Ni–M next-nearest shell was constrained to equal twice that of the Ni–O nearest shell. The RSF and the back Fourier transform spectrum (q-space) of the first two shells of the as-prepared Ni/Mg(Al)O and the fitting data are shown in Figure 4 and Table 2. Agreement in both R and q space for the as-prepared Ni catalyst was obtained with a two-shell fit, including Ni–O for the first shell and a second shell consisting of separate Ni–Ni and Ni–Mg contributions. The latter contribution was derived using TKATOMS and FEFF6 procedures for 5% Ni in MgO.[20–22] Therefore, it can be concluded that all Ni species are present in octahedral sites in the Mg(Al)O lattice, forming a solid solution. The coordination number of Ni atoms in the

Table 2. Curve Fitting Results for the As-Prepared Ni/MgAl(O) Catalyst

shell	R, Å	N	E_0	σ^2, Å^2
Ni–O	2.09 ± 0.01	6	−4.3 ± 2.0	0.006 ± 0.001
Ni–Ni	2.96 ± 0.06	1 ± 1	−25.6 ± 19.3	0.006 ± 0.003
Ni–Mg	2.96 ± 0.06	11 ± 1	−3.8 ± 3.0	0.022 ± 0.006

(19) Yoshida, T.; Tanaka, T.; Yoshida, H.; Funabiki, T.; Yoshida, S. *J. Phys. Chem.* **1996**, *100*, 2302–2309.

(20) Ravel, B.; Newville, M. *J. Synchrotron Radiat.* **2005**, *12*, 537–541.

(21) Webb, S. M. *Phys. Scr.* **2005**, *T115*, 1011–1014.

(22) Martins, A.; Souza-Neto, N. M.; Fantini, M. C. A.; Santos, A. D.; Prado, R. J.; Ramos, A. Y. J. *Appl. Phys.* **2006**, *100*, 13905/101395/6.

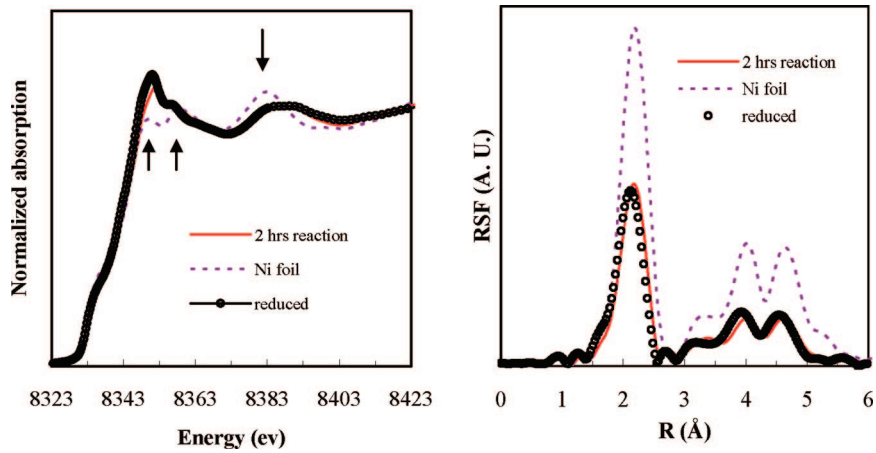

Figure 5. Ni K-edge XANES spectra (left) and RSF (right) of Ni/Mg(Al)O catalyst reduced and after 2 h of reaction, with Ni foil as a reference.

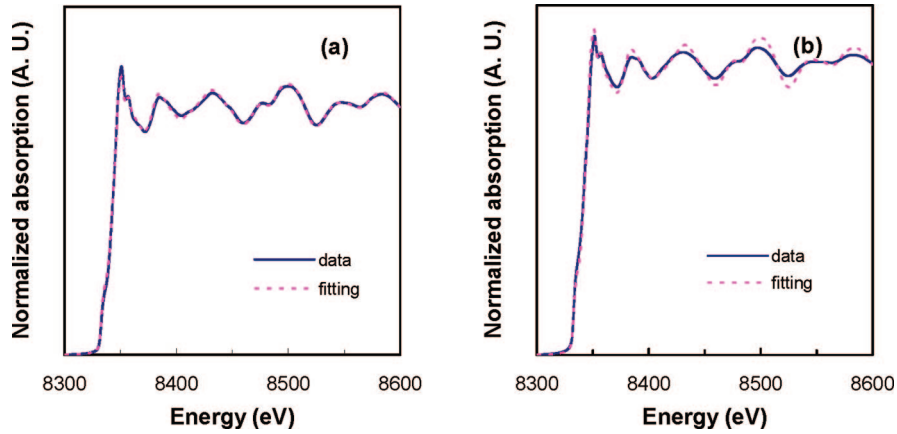

Figure 6. Least-squares fitting of X-ray absorption spectra of Ni/Mg(Al)O catalyst: (a) reduced at 700 °C for 2 h; (b) after 2 h reaction at 500 °C.

Table 3. Results of Least-Squares Fitting of Ni XANES Spectra of Ni/MgAl(O) Catalyst

items	Ni foil	as-prepared Mg(Ni)O	NiO	reduced chi squared
reduced	0.65	0.21	0.13	1.9×10^{-4}
	0.69	0.31		2.6×10^{-4}
	0.68		0.32	3.8×10^{-4}
	1			15.3×10^{-4}
after 2 h reaction	0.74	0.20	0.06	3.1×10^{-4}
	0.75	0.25		3.2×10^{-4}
	0.76		0.24	4.8×10^{-4}
	1.0			11.4×10^{-4}

next-nearest shell is much less than the number of Mg atoms but is consistent with the anticipated composition for a random solid solution of 5% Ni in MgO, which should result in 0.6 Ni and 11.4 Mg next-nearest neighbors.

The Ni K-edge XANES spectrum and the RSF from Fourier transformation of the k^3-weighed EXAFS of Ni/Mg(Al)O after reduction in H_2 and after dehydrogenation of ethane for 2 h at 500 °C, together with the spectral data for a Ni foil, are shown in Figure 5. The RSF of the reduced Ni/Mg(Al)O and the reacted catalyst are similar to those of Ni foil, but the intensities of the first Ni–Ni shell in the RSFs of the catalyst samples are much lower, indicating the presence of some oxidized Ni in the catalysts. To quantify the degree of reduction, least-squares fitting of the XANES spectra of reduced and reacted Ni/Mg(Al)O was conducted by using SixPack software. The fitting components include the XANES spectra for Ni foil, NiO, and the as-prepared catalyst, representing respectively metallic nickel in the catalyst particles, reoxidized Ni on their surfaces, and unreduced Ni in the Mg(Al)O lattice. The fitting results are shown in Figure 6 and Table 3, which lists results for alternative fits as well as for the optimum fit. The catalyst after 2 h of ethane dehydrogenation shows somewhat more metallic Ni (~75%) than the as-reduced catalyst (~65%). However, the amount of reoxidized Ni in the reacted catalyst is much less significant, which suggests that the formation of CNT after ethane dehydrogenation reaction may protect Ni particles from reoxidation due to exposure to air, supporting the tip-growth mechanism. There is no evidence of the formation of nickel carbide after 2 h of the ethane dehydrogenation reaction.[23,24]

Mössbauer spectra were collected at room temperature for the Fe–Ni/MgAlO catalyst as-prepared, after reduction at 700 °C for 2 h, and after ethane dehydrogenation at 650 °C for 8 h. The spectra are shown in Figure 7. The Mössbauer parameters and the contributions of the various iron species identified by least-squares analysis of the spectra are summarized in Table 4. The spectrum recorded of the as-prepared catalyst consists of two quadrupole doublets, indicating two distinct ferric iron species. The doublet

(23) Takenaka, S.; Ogihara, H.; Otsuka, K. *J. Catal.* **2002**, *208*, 54–64.
(24) Takenaka, S.; Kato, E.; Tomikubo, Y.; Otsuka, K. *J. Catal.* **2003**, *219*, 176–185.
(25) Shen, J.; Guang, B.; Tu, M.; Chen, Y. *Catal. Today* **1996**, *30*, 77–82.
(26) Kawabata, T.; Fujisaki, N.; Shishido, T.; Nomura, K.; Sano, T.; Takehira, K. *J. Mol. Catal. A: Chem.* **2006**, *253*, 279–289.
(27) Pattek-Janczyk, A.; Miczko, B.; Morawski, A. W. *Appl. Catal., A* **1996**, *141*, 1–16.
(28) Polychronopoulou, K.; Bakandritsos, A.; Tzitzios, V.; Fierro, J. L. G.; Efstathiou, A. M. *J. Catal.* **2006**, *241*, 132–148.

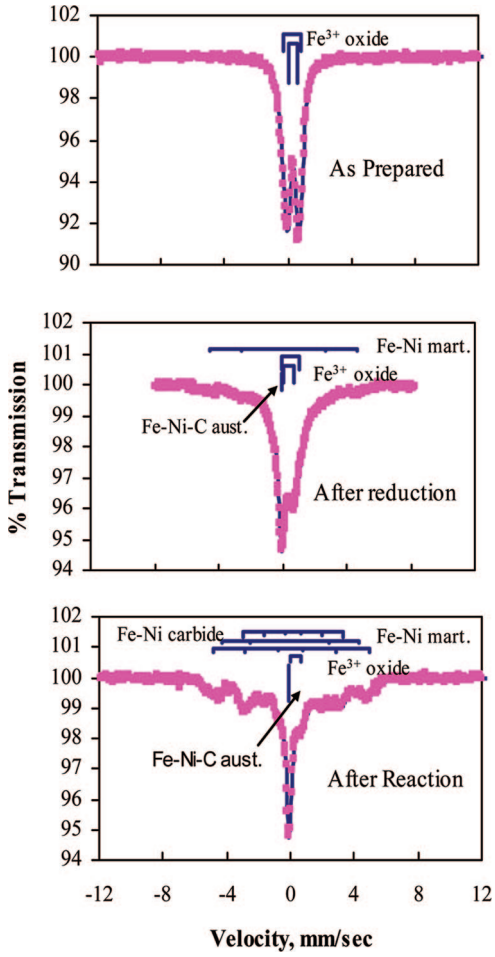

Figure 7. Mössbauer spectra of the Fe–Ni/Mg(Al)O catalyst: as-prepared; after reduction at 700 °C for 2 h; after the ethane dehydrogenation reaction at 650 °C for 8 h.

with the smaller quadrupole splitting is attributed to Fe^{3+} incorporated into the Mg(Al)O lattice, forming a Mg–Ni–Al–Fe–O complex with Fe^{3+} in an asymmetric environment.[25–28] The doublet with the larger QS value is attributed to formation of Fe^{3+} clusters on the surface of support.[26]

After reduction, only about 20% of the iron in the FeNi/Mg(Al)O catalyst is present in metallic form. The broad magnetic sextet is derived from the formation of a magnetic Fe–Ni (bcc) alloy (13%), while the sharp single peak indicates the formation of an austenitic Fe–Ni–C (fcc) alloy phase (7%). A significant percentage of the Fe remains as ferric oxide, although the component with the larger QS may contain a small admixture of Fe^{2+}.

After the ethane dehydrogenation reaction, the Mössbauer spectrum consists of two broad magnetic sextets derived from an Fe–Ni martensitic (bcc) alloy (33%) and a sharp single peak from an Fe–Ni–C (fcc) austenitic alloy (19%). The sextet with the smallest magnetic hyperfine field (H_0 = 193 kG) can be assigned to Fe(Ni) carbide (19%). The remaining absorption (29%), which has been fitted as two very broad (width = 1.9 mm/s) quadrupole components, most likely results from superparamagnetic (spm) Fe–Ni oxide with a spin relaxation time close to that of the Larmor precession time.[29] In view of the small Fe–Ni particle size (10–40 nm), much of this oxide may have formed spontaneously on removing the catalyst from the reactor and exposing it to air. These broad quadrupole components may also obscure an absorption doublet associated with the austenite phase due to Fe atoms in the metal that have carbon nearest neighbors. It is likely that the Fe–Ni–C austenite and the Fe–Ni martensite phases are both active metallic phases for ethane dehydrogenation and CNT formation. Catalyst deactivation may be due to the formation of the carbide phase.

Ethane Dehydrogenation. Ethane dehydrogenation was conducted over Ni/Mg(Al)O and Fe–Ni/Mg(Al)O catalysts at temperatures of 500, 650, and 700 °C with undiluted ethane flowing with a space velocity of 600 mL h^{-1} g^{-1}. During noncatalytic thermal cracking, ethane does not decompose at all at 500 °C and decomposes to 22.5 vol % H_2, 10 vol % CH_4, 19.5 vol % ethene, and 48 vol % unreacted ethane at 650 °C. According to the product distribution, a possible reaction pathway for thermal cracking of ethane is proposed as follows: ethane first cracks to ethene and H_2, and then ethene further decomposes to methane and carbon. Some of the carbon can react with H_2 to produce more methane.

$$C_2H_6 \rightarrow C_2H_4 + H_2 \quad (2)$$

$$C_2H_4 \rightarrow CH_4 + C \quad (3)$$

$$C + 2H_2 \rightarrow CH_4 \quad (4)$$

The generally accepted reaction pathways for catalytic ethane dehydrogenation to hydrogen, methane, and surface deposited carbon (C_S) are provided by the following equations:

$$C_2H_6 \rightarrow CH_4 + C_S + H_2 \quad (5)$$

$$C_2H_6 \rightarrow 2C_S + 3H_2 \quad (6)$$

The following reaction is reversible (methane cracking or methanation) depending on the reaction temperature and the catalyst used.

$$C_S + 2H_2 \leftrightarrow CH_4 \quad (7)$$

There is an additional step, the formation of filamentous carbon (C_f), including both fibers and nanotubes (CNT), from surface

Table 4. Mössbauer Parameters of Fe–Ni/Mg(Al)O Catalyst As-Prepared, Reduced, and after Reaction (Spectra Collected at Room Temperature)

catalyst	IS (mm/s)	QS (mm/s)	H_0 (kG)	width (mm/s)	% Fe	ID
fresh	0.33	0.66		0.49	71	Fe^{3+} in oxide
	0.30	1.15		0.49	29	Fe^{3+} in oxide
reduced at 700 °C for 2 h	0.38	0.65		0.60	30	Fe^{3+} in oxide
	0.52	1.07		1.40	50	Fe^{3+}(Fe^{2+}?) in oxide
	0.05		285	1.16	13	Fe–Ni (bcc) alloy
	−0.08			0.30	7	Fe–Ni (fcc) alloy
after reaction at 650 °C for 8 h	0.34	0.58		1.90	29	Fe^{3+} oxide (spm)
	0.01		303	0.79	23	Fe–Ni (bcc) alloy
	0.00		265	0.62	10	Fe–Ni (bcc) alloy
	0.15		193	0.65	19	Fe(Ni)–C carbide
	−0.07			0.34	19	Ni–Fe(C) (fcc) alloy

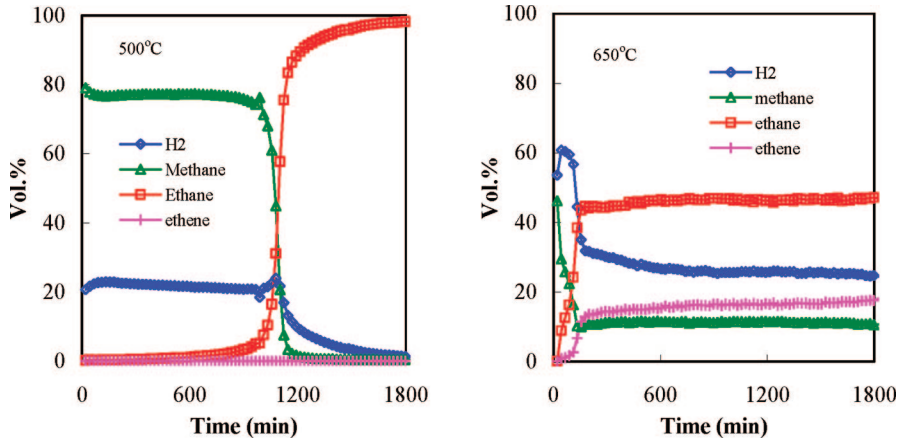

Figure 8. TOS product distribution of ethane dehydrogenation over Ni/Mg(Al)O catalyst at 500 °C (left) and 650 °C (right).

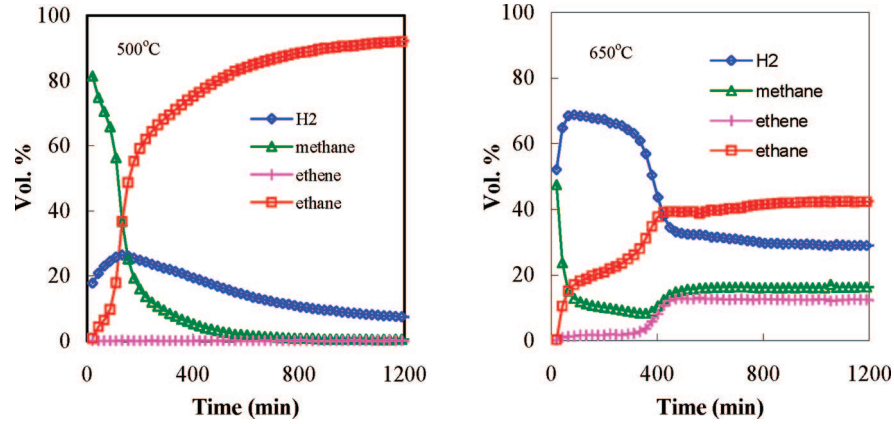

Figure 9. Time-on-stream product distribution for ethane dehydrogenation on Fe–Ni/Mg(Al)O catalyst (Fe:Ni = 65:35) at 500 °C (left) and 650 °C (right).

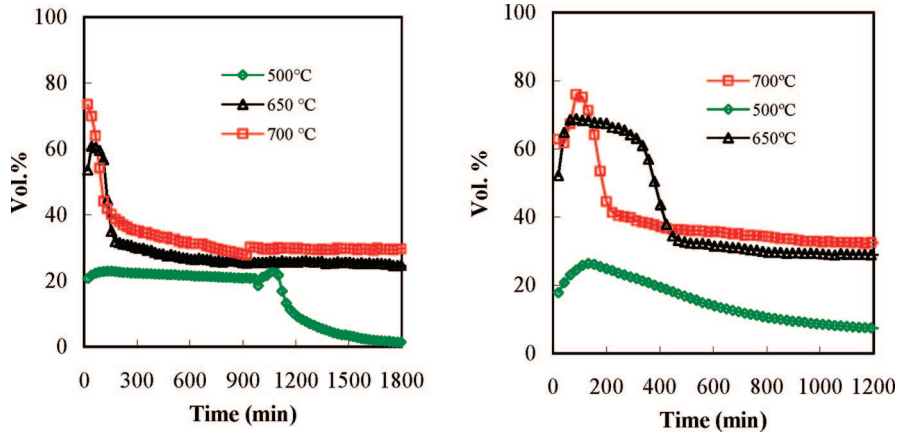

Figure 10. Time-on-stream hydrogen production by ethane dehydrogenation over Ni/Mg(Al)O (left) and Fe–Ni/Mg(Al)O (right) catalysts at different temperatures.

deposited carbon (C_S), determined by the carbon diffusion rate through or around the catalyst particles.[30–32]

$$C_S \rightarrow C_f \tag{8}$$

Figure 8 shows the time-on-stream (TOS) product distribution from ethane decomposition over the Ni/Mg(Al)O catalyst at 500 and 650 °C. At 500 °C, Ni/Mg(Al)O exhibits good catalytic performance. It maintains catalytic activity for over 16 h with almost 100% ethane conversion to ~20 vol % H_2 and 80 vol % methane. Given that 4 times more methane than H_2 is produced at 500 °C, the dominant reaction is reaction 5, producing equal molar C_S, methane, and H_2. Nearly 1/3 of C_S further reacts with H_2 to yield more methane, and the remainder becomes CNT. As discussed later, the CNT produced in this reaction have a stacked-cone nanotube (SCNT) structure. Therefore, the overall reaction of ethane dehydrogenation over Ni/Mg(Al)O catalyst at 500 °C can be expressed as

$$3C_2H_6 \rightarrow 4CH_4 + H_2 + 2C_f \tag{9}$$

(29) Zhao, J.; Huggins, F. E.; Feng, Z.; and Huffman, G. P. *Phys. Rev. B: Condens. Matter* **1996**, *54*, 3403–3407.
(30) Chin, S. Y.; Chin, Y.; Amiridis, M. D. *Appl. Catal., A* **2006**, *300*, 8–13.
(31) Snoek, J.-W.; Froment, G. H.; Fowles, M. *J. Catal.* **1997**, *169*, 240–249.
(32) Snoeck, J.-W.; Froment, G. H.; Fowles, M. *J. Catal.* **1997**, *169*, 250–262.

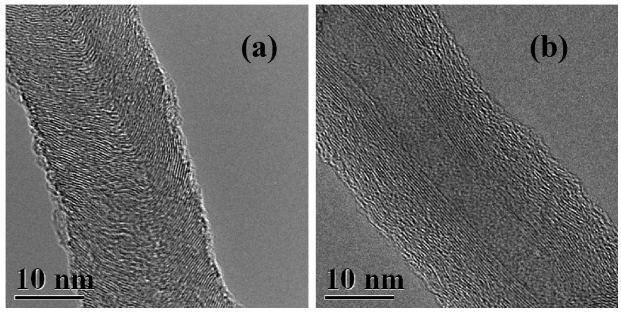

Figure 11. HRTEM images of CNT deposited on FeNi/Mg(Al)O catalyst by ethane dehydrogenation. Reaction temperature: (a) 525 and (b) 650 °C.

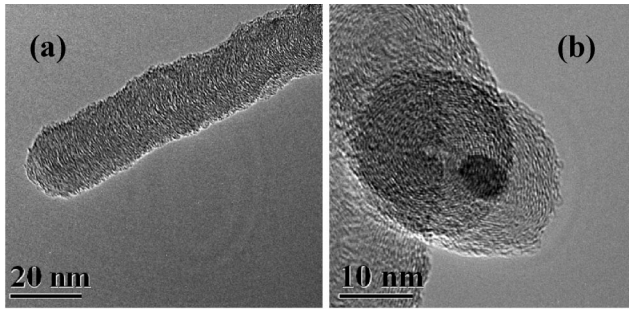

Figure 12. HRTEM images of CNT deposited on on Ni/Mg(Al)O catalyst by ethane dehydrogenation. Reaction temperature: (a) 500 and (b) 650 °C.

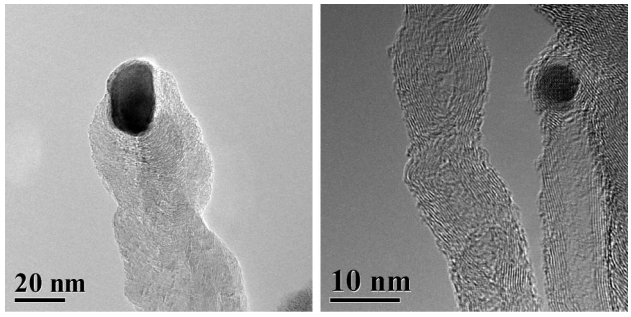

Figure 13. HRTEM images illustrating the tip-growth mechanism of CNT formation. Catalyst particle size determines the diameter of formed CNT. Reaction temperature: 500 °C.

The chemical reaction rate is in equilibrium with the carbon consumption rate from the catalyst surface, including the methanation reaction and C_S diffusion to form SCNT, which allows the catalyst to maintain its activity. After 16.7 h, the available active metal surface of the Ni catalyst particles becomes enclosed in the SCNT, and the catalyst then gradually deactivates.

On further increasing the temperature to 650 °C, methane cracking becomes dominant over the methanation reaction, increasing the H_2 yield. Moreover, buildup of carbon occurs on the surfaces of catalyst particles since the carbon is generated too rapidly to be diffused through the catalyst particles to produce CNT. Thus, the catalyst rapidly loses active sites, and ethane decomposition diminishes to the level of thermal cracking. Ethene is increasingly detected as a product as the catalyst loses its activity at 650 °C.

Figure 9 shows the time-on-stream (TOS) product distribution from ethane decomposition over a bimetallic Fe–Ni/Mg(Al)O catalyst at reaction temperatures of 500 and 650 °C. At 500 °C, the Fe–Ni/Mg(Al)O catalyst shows less activity than that

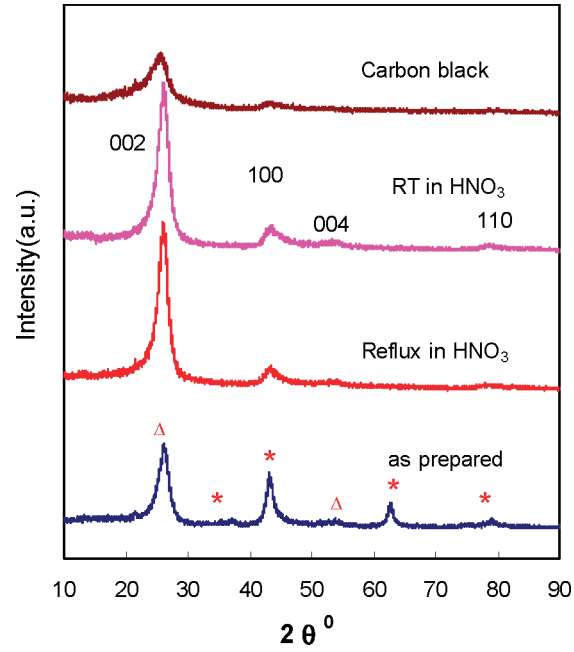

Figure 14. XRD patterns of the CNT as-prepared and of purified CNT both at room temperature and reflux condition. The XRD pattern of carbon black is shown as a reference.

of the Ni/Mg(Al)O catalyst. At the beginning of reaction, it converts ethane completely to 20 vol % H_2 and 80 vol % methane, just as the Ni catalyst does. However, it gradually deactivates to a new equilibrium level of 7.5 vol % H_2, with unreacted ethane as the balance of the product gas.

On increasing the reaction temperature to 650 °C, the Fe–Ni/Mg(Al)O catalyst exhibits a dramatic increase in H_2 production (over 65 vol % H_2 and 10 vol % methane) and maintains its activity for over 5 h before gradually declining to the thermal cracking level. On comparing these data with those of the monometallic Ni/Mg(Al)O catalyst, it is evident that the diffusion of carbon through the Fe–Ni alloy catalyst at 650 °C must be enhanced relative to that of the pure Ni catalyst.

The driving force for carbon diffusion inside the catalyst particles and the formation of filamentous carbon is due to the carbon concentration gradient, arising from the difference in carbon solubility at the gas/catalyst particle surface and CNT/catalyst particle surface.[31,33] At steady state, the rates of the ethane decomposition reaction, net surface reaction, and carbon diffusion through the catalyst particle are equal. At 650 °C, the carbon diffusion rate in bimetallic Fe–Ni/Mg(Al)O is apparently much faster than that in monometallic Ni/Mg(Al)O catalyst. Thus, the former can maintain steady-state operation for a reasonable period of time, but the latter deactivates quickly during reaction. Hence, inclusion of the second metal to form a metal alloy can significantly change the carbon diffusivity or solubility inside the catalyst particles at elevated temperatures, prolonging catalyst lifetime.[34] Catalyst deactivation after a period of steady-state operation may be due to the formation of a new phase, metal carbide, which lowers the solubility of carbon at the gas/catalyst particle surface or the diffusion coefficient of carbon atom through the catalyst particle. For example, the diffusion coefficient of carbon through Fe_3C is 10^4 times lower than that through austenite,[35] which significantly lowers the

(33) Rostrup-Nielsen, J. R.; Trimm, D. L. *J. Catal.* **1977**, *48*, 155–165.
(34) Baker, R. T. K. *Carbon* **1989**, *27*, 315–323.
(35) Reshetenko, T. V.; Avdeeva, L. B.; Ushakov, V. A.; Moroz, E. M.; Shmakov, A. N.; Kriventsov, V. V.; Kochubey, D. I.; Pavlyukin, Y. T.; Chuvilin, A. L.; Ismagilov, Z. R. *Appl. Catal., A* **2004**, *270*, 87–99.

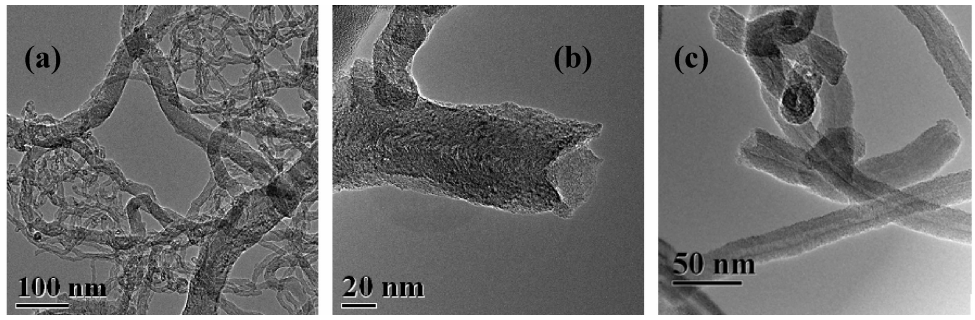

Figure 15. TEM images of (a, b) purified SCNT produced by ethane decomposition using the Ni/Mg(Al)O catalyst (500 °C, 40 h) and (c) purified MWNT produced by using the Fe–Ni/Mg(Al)O catalyst (650 °C, 8 h).

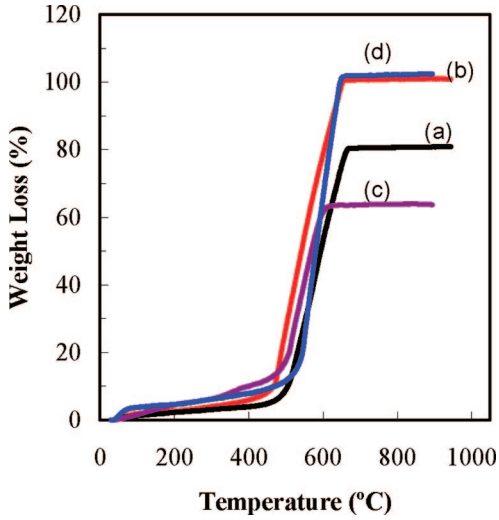

Figure 16. Thermal gravimetric analysis of the SCNT and MWNT as-prepared and purified in 6 M HNO_3 for 2 h under reflux condition: (a) as-prepared SCNT; (b) purified SCNT; (c) as-prepared MWNT; (d) purified MWNT.

driving force for carbon diffusion. Additionally, gas access to the catalyst particles is gradually reduced by enclosure within CNT, as noted earlier.

Figure 10 summarizes the TOS H_2 production over the Ni/Mg(Al)O and bimetallic FeNi/Mg(Al)O catalysts at 500, 650, and 700 °C. The Ni/Mg(Al)O catalyst has the longest lifetime at 500 °C. It maintains catalytic activity for 16.7 h with 100% ethane conversion, but the H_2 selectivity is only 25%, and the net gain of hydrogen during this period of time is 3316 mL/g catalyst. At 650 and 700 °C, the monometallic Ni catalyst deactivates quickly. The bimetallic FeNi/Mg(Al)O catalyst shows high H_2 selectivity and activity at 650 °C, at which temperature H_2 generation is ~65 vol % and is maintained for over 5 h. The net gain of hydrogen till deactivation at 470 min is about 4418 mL/g catalyst. At 700 °C, both the Ni catalyst and the Fe–Ni catalyst deactivate very quickly, but the Fe–Ni catalyst exhibits a higher H_2 yield.

TEM Characterization of CNT. The morphology of the CNT produced over Mg(Al)O supported catalysts was investigated using high-resolution transmission electron microscopy (HRTEM). Figure 11 shows the CNT structures produced by ethane decomposition over Fe–Ni/Mg(Al)O catalyst at reaction temperatures of 525, and 650 °C. The structure of CNT is very sensitive to reaction temperature. At 525 °C, the CNT have a stacked-cone nanotube structure (SCNT), and at 650 °C, they are predominantly concentric parallel-walled MWNT. Figure 12 shows the structure of CNT produced over the Ni/Mg(Al)O catalyst at temperatures of 500 and 650 °C. At 500 °C, the CNT are essentially all SCNT. However, at 650 °C, an onionlike structured carbon soot is formed together with filamentary carbon. The formation of the onionlike carbon soot was also observed by Nolan et al.[36] on supported Ni and Co particles at 600 °C for CO disproportionation reaction.

The formation of MWNT and SCNT over bimetallic Fe–M (Ni, Mo, Pd) catalysts supported on γ-Al_2O_3 was discussed previously.[2] The CNT nanostructures grow away from the surfaces of the binary catalyst particles because they are anchored to the alumina support by the formation of hercynite ($FeAl_2O_4$). However, the catalyst particles supported on Mg(Al)O exhibit a tip-growth mechanism of CNT formation. This is illustrated by Figure 13, which shows metal catalyst particles at the tips of CNT formed by ethane dehydrogenation over Ni/Mg(Al)O and Fe–Ni/Mg(Al)O catalysts at 500 °C. Such structures have also been observed, for example, by Dai et al. using a patterned catalyst array.[37] It is generally agreed that formation of CNT by CCVD involves three steps, consisting of the formation of surface carbon C_S, the dissolution and diffusion of the C_S through the catalyst particle, and the nucleation of carbon filaments.[38] Because of different interactions between catalyst metal particles and the support, the catalyst particles either move forward to the tips of the nanotubes while the CNT are generated on the rear (tip-growth mechanism) or remain attached to the support while the CNT grow away from the anchored particles (base growth mechanism). Tip growth would appear to have advantages for our application, which is focused on producing large quantities of hydrogen and nanotubes. The metal particles move away from the support and form a loosely connected aggregate of CNT inside the reactor. Moreover, it favors the formation of CNT with open ends, making the CNT produced easier to clean.

CNT Purification. The carbon product from ethane decomposition was collected after reaction and treated in 6 M HNO_3 to remove the catalyst. The reaction was carried out either at room temperature for 2 h or in hot 6 M HNO_3 solution under reflux for 2 h. Figure 14 shows the XRD patterns of the CNT as-prepared after 40 h reaction at 500 °C on Ni/Mg(Al)O, the CNT after HNO_3 treatment, and carbon black for reference. The CNT as-prepared show a large graphite peak at $2\theta = 26°$ (marked with a triangle) and peaks from the Mg(Al)O support (marked with a star). After treatment in 6 M HNO_3 solution, the XRD patterns show only the graphitic peaks as indexed,[39] establishing that high-purity CNT can be obtained by this mild acid treatment. Figure 15 shows typical TEM images of purified SCNT (by cold HNO_3 solution) produced by ethane dehydro-

(36) Nolan, P. E.; Lynch, D. C.; Culter, A. H. *Carbon* **1994**, *32*, 477–483.
(37) Dai, H. *Acc. Chem. Res.* **2002**, *35*, 1035–1044.
(38) Bhushan, B. *Springer Handbook of Nanotechnology*; Spinger-Verlag: Berlin, 2004; pp 59–63.
(39) Li, W.; Liang, C.; Zhou, W.; Qiu, J.; Zhou, Z.; Sun, G.; Xin, Q. *J. Phys. Chem. B* **2003**, *107*, 6292–6299.

genation at 500 °C over a Ni/Mg(Al)O catalyst and MWNT prepared over an Fe-Ni/Mg(Al)O catalyst at 650 °C. No catalyst particles are observed, and the nanotubes exhibit open ends, typical of CNT formed by the tip-growth mechanism, which leaves the metal catalyst particles accessible to the acid solution. Thermal gravimetric analysis shown in Figure 16 establishes that the residue of as-prepared SCNT is 17.15 wt % and that of the as-prepared MWNT is 36.2 wt %, while the residues of purified SCNT and MWNT are both close to 0. The major weight loss occurs over the temperature range from 450 to 650 °C for all samples. After cooling the samples to room temperature, the purities of purified CNT could be determined more accurately and were found to be 99.5% for the SCNT and 99.6% for the MWNT.

4. Summary and Conclusions

Mg(Al)O supports prepared by calcination of Mg–Al hydrotalcite with a Mg/Al molar ratio of 5 consist of MgO nanocrystal agglomerates with large surface areas. Ni and Fe–Ni catalysts were dispersed onto the Mg(Al)O support by an incipient wetness method followed by calcination at 550 °C for 5 h. The catalysts were first reduced in hydrogen at 700 °C for 2 h and then reacted with undiluted ethane. Catalytic dehydrogenation of ethane was carried out at temperatures ranging from 500 to 650 °C over both types of catalyst. The principal results are summarized below:

1. At 500 °C, the Ni/Mg(Al)O catalyst was highly active and very stable with 100% conversion of ethane to 20 vol % H_2 and 80 vol % methane. It exhibited no loss of activity for over 16.7 h at a space velocity of 600 mL h^{-1} g^{-1} of undiluted ethane. The CNT were all in the form of SCNT.

2. The Fe–Ni/Mg(Al)O exhibited its best catalytic behavior at 650 °C, at which temperature it was active for over 5 h, yielding 65 vol % H_2, 10 vol % CH_4, and 25 vol % unreacted ethane.

3. At 500 °C, the CNT structure produced over the Ni/Mg(Al)O catalyst was stacked-cone nanotubes (SCNT). Increasing the temperature to 650 °C led to an onion soot/fiber mixture that rapidly deactivated the catalyst.

4. The CNT formed over the Fe–Ni/Mg(Al)O catalyst changed with temperature from SCNT (525 °C) to parallel-walled MWNT (650 °C).

5. TEM and STEM established that the reduced catalysts consisted of metallic nanoparticles 8–40 nm in size dispersed on the Mg(Al)O. XAFS and Mössbauer spectroscopy established that the active phases were metallic Ni and Fe–Ni alloys, although significant oxide phases were also present. Both austenitic Fe–Ni–C and martensitic Fe–Ni alloy phases were observed in the Fe–Ni catalyst after reaction.

6. The presence of Ni and Fe oxides after reduction and reaction is due to incomplete reduction and/or reoxidation on exposure to air. The oxides were identified by Ni XAFS spectroscopy and ^{57}Fe Mössbauer spectroscopy.

7. The CNT were formed by a tip-growth mechanism over the Mg(Al)O-supported catalysts and were easily purified by a one-step 6 M nitric acid treatment.

Acknowledgment. This research was supported by the U.S. Department of Energy, Office of Fossil Energy, under DoE Contract DE-FC26-05NT42456. XAFS spectroscopy was performed at the National Synchrotron Light Source, Brookhaven National Laboratory, which is supported by U. S. DoE under contract No. DE-AC02-98CH10886.

EF7004018